# A Content-Adaptive Method for Fractional Image Rescaling Based On Constrained Seam Carving

Yijun Xiao, J. Paul Siebert, W. Paul Cockshott

***Abstract*— In the digital cinema postproduction chain, image rescaling serves as a core function. The quality of rescaling is critical to maintaining the visual impact of a digital film at play-out. In the EU funded project IP-RACINE, it is required to address color distortion, artifacts and image blur in fractional rescaling within 1 pixel for a typical image of resolution 2K. To this end, we proposed a hybrid warping framework for fractional image rescaling that not only unifies the two dominant image rescaling methods, namely discrete mapping and interpolation, but also offers greater flexibility in preserve properties of image contents. Within this framework we have devised a novel rescaling method based on constrained seam carving. Compared with unconstrained seam carving[1], the new method can preserve global geometry of image contents and confine nonlinear distortion to be within $\pm 1$ pixel; compared with nearest neighbour mapping, it generates less visible artifacts; compared with interpolation methods, it can maintain color fidelity and sharpness in the original image.**

***Index Terms*—Image rescaling, Digital cinema, Seam carving, Hybrid warp, Shape preserving.**

## I. Introduction

Film or cinema is a major driving force for the entertainment industry. Commanding large scale financing, this medium employs the state-of-the-art in production/ postproduction technology to achieve the most exacting visual quality. The whole cine chain from capture to play-out is now fast moving towards all digital form due to the recent advances in imaging sensor technology matched by the affordability of the necessary computing resources. In response to this trend, European Union has established a large project named IP-RACINE (short for Integrated Project Research Area Cinema), aiming to “create a technology chain and workflow that allow the European digital cinema industry to deliver a complete experience from scene to screen”. The University of Glasgow has been collaborating in this project investigating cine image compression and rescaling. One of the requirements in IP-RACINE is to address image degradation that results from a small scale resizing operation (termed as fractional rescaling). The industrial partners in the project reported that they can observe colour distortion, image blur, and visible artefacts when using conventional image rescaling methods in fractional scale.

Manuscript received Jan. 7, 2008. This work was supported by the European Commission under the IP-RACINE project (IST-2-511316-IP).

Yijun Xiao, J. Paul Siebert and W. Paul Cockshott are with Department of Computing Science, University of Glasgow, G12 8QQ, United Kingdom (email: {yjxiao,psiebert,wpc}@dcs.gla.ac.uk)

Given this context, the Glasgow University team has analyzed systematically two sets of commonly-used rescaling methods: discrete mapping and interpolation methods. We observed that the discrete mapping methods are able to preserve image sharpness (and colour fidelity for colour images) although inevitably introducing geometrical aliasing in rescaled images. On the other hand, although interpolation methods aim to preserve geometry of image contents, nevertheless they cause images to be smoothed thereby losing some fine image details. To our best knowledge, the problem of preserving both image sharpness and geometry in fractional image rescaling has not yet been systematically studied in the literature. Therefore to advance the state-of-the-art in fractional image rescaling, it is important to investigate the sharpness-geometry trade-off problem.

This paper reports our study in fractional image rescaling, and is organized as follows: section II reviews the major lines of research in image rescaling in the literature and then analyses the quality degradation specifically in fractional scale. Based on the analysis, a hybrid warping scheme is proposed as a framework for image rescaling to alleviate quality degradation. Following this framework, Section III then discusses a novel rescaling method based on seam carving which aims to generate less visible artifacts. Some experimental results are shown and discussed in Section IV and conclusions are drawn in Section V.

## II. Analysis of Image Rescaling

### A. Overview of Image Rescaling

Image rescaling (image resizing) plays a major role in image manipulation. In addition to its direct use, image rescaling is of fundamental importance to many computer vision and image processing algorithms such as image warping [2], pyramid construction [3], image-based rendering [4], etc. The process of image rescaling involves a re-sampling that transforms the pixels on the grid of the original image to the pixels on a new grid representing the rescaled image. Depending on the scale, techniques for image rescaling can be very different. For instance, for octave image shrinking (rescaled to $1/2^n$ of the original scale), convolution-based techniques are well justified because similar processes occur in human vision [5] and their implementation is relatively simple. For octave image expansion (rescaled to $2^n$ of the original scale), super-resolution techniques such as reconstruction-based [6, 7] or synthesizing-based [8, 9] methods may be required to generate plausible extra visual information associated with the enlarged scale.

However, for a rescaling operation at an arbitrary scale, i.e. a scale that lies between two octave scales (termed as a *fractional* scale in this paper), the rescaling methods which work effectively for octave rescaling appears to be less effective because the patch-based computational formalism involved in those methods is difficult to adapt to an arbitrary scale. More versatile methods such as discrete mapping and interpolation methods seem to be more appropriate to fractional rescaling.

The simplest and most popular discrete mapping method, the nearest neighbour mapping, can be also considered to be a 0-order polynomial interpolation. Therefore in the literature, some researchers use the term “image interpolation” and “image rescaling” interchangeably. However in this paper, we distinguish image interpolation and image rescaling because interpolation is not necessarily the only means of rescaling an image. In the later part of the paper, we propose a new warping scheme which can be considered as a more general method to rescale images.

Numerous methods have been proposed for image interpolation from different perspectives. For instance in the signal processing community, image interpolation is interpreted as the process of reconstructing the signal and its subsequent re-sampling [10, 11]. However, for Computer Graphics and CAD researchers, image interpolation is often regarded as a means to reconstructing the image surface, usually assumed to be continuous, therefore interpolants which exhibit good differential properties such as polynomials [12, 13] are preferred.

Although different interpolation methods yield different qualities of rescaled images due to the different mathematical properties of the interpolants employed, it is yet hard to claim any one method outperforms all others. In practice the selection of image interpolation methods usually depends on task-specific properties [14]. Nevertheless, some good methods, such as Bilinear and Bicubic interpolation (1-order and 3-order polynomial interpolation) have proven popular because they often generate results of acceptable quality and are found to be numerically stable.

### *B. Image Degradation in Fractional Rescaling*

Many image rescaling methods yield degradation in visual quality. A large volume of work has been published to address image degradation in rescaling, including earlier work in choosing different interpolants (as mentioned in Section II.A). More recent methods adapt dynamically to image contents [15, 16] where local and global structures are learnt to supervise image representation in a way that the rescaled image looks better to human observers.

In this paper, we limit our discussion to fractional rescaling, in which image degradation occurs primarily in the form of blurring or geometrical aliasing. The blurring arises when a well-focused digital cine picture is subjected to a very small change in scale, say 5%. When such a small-scale change is applied, the image details that have spatial frequencies near the Nyquist limit in the original image will be incremented with phase shifts that cause the signal to pass in and out of representability of the new pixel grid. Figure 1 gives an example of this blurring effect, where a test image with repeated 1-pixel stripe pattern was enlarged by 5% using bilinear and bicubic interpolation. It is clearly seen that the resultant images are significantly blurred.

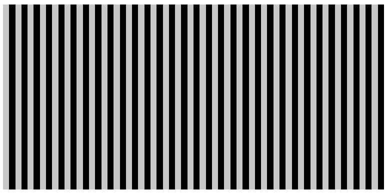

(a) Test image with repeated patterns

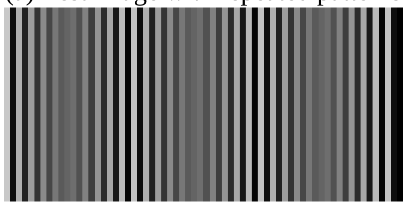

(b) Enlarge image in (a) by 5% using bilinear interpolation

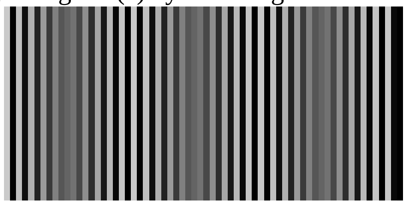

(c) Enlarge image in (a) by 5% using bicubic interpolation

Figure 1 Blurring effect in fractional rescaling

Another form of image degradation is manifest as geometrical aliasing when discrete mapping methods are applied. An example is illustrated in Figure 2, where “zigzag” artifacts occur in image expansion using nearest neighbor mapping. The reason for this aliasing is also the phase shift due to fractional rescaling, which causes spatial quantization errors of the pixel grid of the rescaled image.

While the Nyquist-Shannon sampling theorem tells us that some degradation is inevitable with fractional image rescaling, in practice the best we can do may well be to make image degradation less visually intrusive to the user. In other words, we have to alter the image degradation in such a way that is less visible to the human visual system and this is the core principle underpinning adaptive image rescaling methods [15, 16]. In the next section, we propose a general framework for fractional image rescaling that transforms image degradation using a hybrid warp.

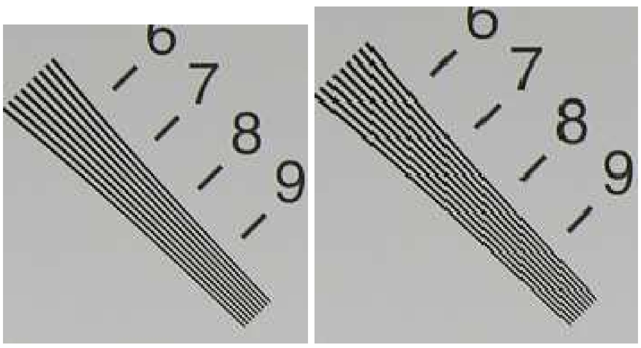


(a) test image; (b) 5% enlarged image by nearest neighbor mapping

Figure 2 Geometrical aliasing in fractional rescaling

### C. A General Framework for Fractional Rescaling

As explained in Section II-B, image degradation caused by signal phase shifting in fractional rescaling is inevitable and we may alter the form of degradation to make it less visible. A first question is whether image degradation is transformable. If the answer is yes, then we may be able to tune the image degradation according to a specific need. Let us assume a rescaled image can be obtained from an interpolated surface of the original image:

$$I_s(m,n) = f(x,y) \tag{1}$$

where $f$ is the interpolated surface of original image $I(i,j)$. In traditional image interpolation, the new image $I_s$ is obtained by sampling the interpolated surface $f$ at the positions linearly transformed from pixel indices $(m,n)$:

$$x = m/\lambda_x,\ y = n/\lambda_y \tag{2}$$

where $\lambda_x$, $\lambda_y$ are scaling factors on dimension $x$ and $y$ respectively.

A traditional way of looking at Eq(1) is that a better rescaling may be achieved by obtaining a better-behaved interpolated surface $f$. This idea has led the study of different interpolants including 0-order, 1-order and 3-order polynomials (that give nearest neighbour mapping, bilinear and bicubic interpolation respectively). Many other interpolants have been reported in the literature, such as quadratic [13], sinc [11], spline [17], wavelet [18], etc., nevertheless, there is a limit to this line of investigation as discussed in Section II-B.

Another way of looking at Eq(1) is that it represents a discrete warping function. If Eqs(2) hold true, then the warp in Eq(1) is a linear warp. From this point of view, all previous image interpolation methods assume a linear warp. Since it is difficult to attack the theoretical limit set by Nyquist-Shannon theorem using a linear warp, we believe a nonlinear warp has the potential to achieve better results. Based on this idea, we alter Eqs(2) to the following:

$$x = m/\lambda_x + \delta_x,\ y = n/\lambda_y + \delta_y \tag{3}$$

Eqs(3) represent a hybrid warp that increments the linear warp of Eq(2) with a displacement map $(\delta_x,\delta_y)$. Eqs(3) then have the flexibility to be linear or nonlinear depending on $(\delta_x,\delta_y)$. For instance, if $(\delta_x,\delta_y)$ is nonlinear to $(m,n)$ then Eqs(3) exhibit nonlinear properties. The mechanism expressed by Eq(1) and Eqs(3) is powerful as it not only provides greater flexibility to generate rescaled images but also unifies many existing image rescaling methods. For instance, an interpolation can be obtained if $\delta_x=0$ and $\delta_y=0$, and a nearest neighbor mapping can be achieved if:

$$\begin{aligned} \delta_x &= round(m/\lambda_x) - m/\lambda_x \\ \delta_y &= round(n/\lambda_y) - n/\lambda_y \end{aligned} \tag{4}$$

In Eqs(4), round(·) denotes a rounding function which outputs the integer closest to its input variable.

This is an interesting observation. If we adjust $(\delta_x,\delta_y)$ within their upper and lower bounds in Eqs(4), we can generate a rescaled image "blended" between an interpolation and nearest neighbour mapping. This observation inspired us to consider the hybrid warp defined in Eq(1) and Eqs(3) to be capable of transforming image degradation. In our investigation, we found this hypothesis to hold. The next section presents a method of adjusting $(\delta_x,\delta_y)$ that transforms the geometrical aliasing in a discrete mapping.

## III. PROPOSED ALGORITHM

$(\delta_x,\delta_y)$ in Eqs(4) exhibit regular zigzag patterns. This is the reason for aliasing in nearest neighbor mapping as shown in Figure 2(b). To make the aliasing artefacts less noticeable, $(\delta_x,\delta_y)$ must be adapted to the local image structure or contents. To this end, we have devised a content-adaptive discrete mapping method based on the seam carving techniques proposed in *SIGGRAPH* 2007 [1].

The original seam carving method [1] is a nonlinear warp that can also be represented by Eq(1) and Eqs(3). While demonstrating its content-aware ability in image resizing, the original seam carving method introduces evident geometrical distortion of image contents because there is no constraint imposed on the range of $(\delta_x,\delta_y)$ causing uncontrolled nonlinearity of the warp. To address this issue, we have introduced constraints to control nonlinearity caused by seam operations.

Let us first briefly explain the concept of a seam. Assume we have an image *I(i,j)* and its corresponding energy map *E(i,j)*, a seam is defined as a connected path of pixels along one image axis (vertically or horizontally). For instance, a vertical seam can be expressed as follows (a horizontal seam can be expressed similarly):

$$\begin{aligned} &\mathbf{s}_V = \{(s(j), j)\}_{j=1}^{H}, s(j) \in [1,2,\ldots,W] \\ &s.t.\ \forall j, |i(j) - i(j-1)| \le 1 \end{aligned} \tag{5}$$

where $\mathbf{s}_v$ denotes the vertical seam, $W$ and $H$ represent width and height of the image measured by number of pixels, and $(s(j), j)$ forms a pair of horizontal and vertical coordinates of a pixel of the seam.

Note that there are two constraints on a seam defined in Eq(5). The first is a connectivity constraint, i.e., two adjacent pixels in a seam must be constrained in a 8-neighbourhood. The second is a functional constraint, i.e.., that $s(j)$ is a function of $j$, which implies that the seam has only one pixel in each row of the image. These constraints have influence on the effects of seam operations (insertion and removal). The connectivity constraint guarantees a seam to be discretely connected, thereby affecting the image "continuously". The functional constraint ensures that one operation on a seam affects the image by only one pixel across (expanded or shrunk by one pixel in width or height) therefore causing maximally $\pm 1$ shifts of pixels.

An optimal seam is considered as the one that minimizes its energy (sum of energy of its pixels):

$$\mathbf{s}^* = \min_{\mathbf{s}} E(\mathbf{s}) \tag{6}$$

Based on the definitions above, image rescaling can be performed by simply repeating the operation of removing or inserting optimum seams. The intuition here is that operation of a minimum energy seam will introduce least visual intrusion to the image.

The problem of geometrical distortion may become evident following the original seam carving [1]. Figure 3(b) illustrates highly perceptible geometrical distortion of image contents, where the displayed image was derived from the test image in Figure 3(a) by shrinking 50 pixels horizontally using the original seam carving algorithm. The resized image was then stretched back to its original size using a linear warp (bilinear interpolation) in order to illustrate the shifts of image contents. As it can be seen in Fig. 3(b), the distortion is obvious. For instance, the green and red peppers on the left part of Figure 3(b) look smaller in width than those in image Figure 3(a).

(a)

(b)

(c)

Figure 3. Comparison of geometrical distortion in seam carving method: (a) pepper image (198x135); (b) image shrunk to (148x135) by the original seam carving [1] and stretched back to (198x135) using a linear warp; (c) image shrunk to (148x135) by constrained seam carving and stretched back to (198x135) using a linear warp.

The reason for manifest geometrical distortion in Fig. 3(b) is that there is little constraint on forming the seams. The selected seams to be removed or inserted can be at arbitrary locations as long as they do not violate the definition in Eq(5). Because of the huge freedom given to such seams, the original seam carving algorithm does not allow control over the overall level of nonlinearity in seam operations. To illustrate this, we map the pixels in Figure 3(b) back to the corresponding pixels in Figure 3(a), and then calculate shifts $\delta_x$ between corresponding pixels (only $\delta_x$ was calculated because the image was rescaled only horizontally). Figure 4(a) shows the shifts selected in the 50-th and 100-th rows. It can be seen that the shifts exhibit an apparent nonlinearity with the largest shift being about 15 pixels, giving rise to noticeable geometrical distortion in the resultant image.

To reduce geometrical distortion in seam carving we must constrain the nonlinearity of seam operations. While a seam operation inevitably introduces nonlinearity by its nature, it may be possible to control the level of nonlinearity caused by seam operations.

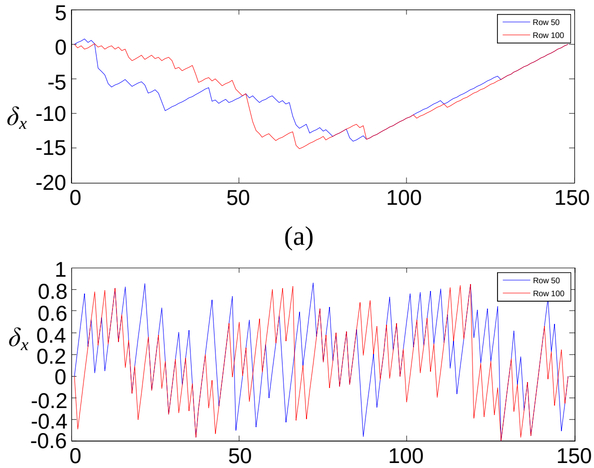


(b)

Figure 4 (a) Pixel shift measured on row 50 and row 100 of image in Figure 3(b); (b) Pixel shift measured on row 50 and row 100 of image in Figure 3(c)

The basic idea is to limit the seam search range and the number of seams constructed within that range. An operation on a seam involves shifts of $\pm 1$ pixel for the pixels within the bounding rectangle of the seam, i.e. the minimum rectangle that contains the seam. Because there is no constraint on the seam rectangular bound in the original seam carving method, in the worst case, this bound can be as big as the whole image, that is to say, the whole image will be affected by shifts of $\pm 1$ pixel. When more seam operations are applied, the shifts of pixels then build up, since the seam bounding rectangles may overlap, and this explains the nonlinear property illustrated in Figure 4.

Based on the analysis above, we propose a constrained version of seam carving for fractional image rescaling. In the constrained seam carving, the whole image is divided into $n_r$ non-overlapping vertical (or horizontal) regions uniformly, where $n_r$ is the number of pixels the image expands (or shrinks) horizontally (or vertically). Each region allows only one seam operation, thereby limiting shifts of image contents to be within $\pm 1$ pixel in that region. Because the divided regions do not overlap, the rectangular bounds of seams in different regions do not overlap as well. Therefore the shifts caused by seam operations in different regions do not accumulate together. When all the regions are combined together to form the complete rescaled image, the global image content structure remains proportional to that of the original image because the regions are divided uniformly. While nonlinear distortion has been introduced within each region, this distortion has been bounded to a shift of $\pm 1$ pixel for each pixel. Figure 5 illustrates the principle of constrained seam carving, where the test image in Figure 3(a) has been divided into 5 uniform regions and one seam has been constructed in each region.

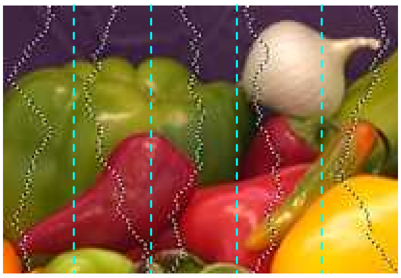

Figure 5 Constrained seam carving

When we apply the constrained seam carving to the test image in Figure 3(a), we generate the rescaled image shown in Figure 3(c). In this case the test image was shrunk by 50 pixels horizontally and then stretched back to its original size. It can be seen that the result in Figure 3(c) exhibits much less geometrical distortion than that in Figure 3(b) where the original seam carving was applied. To determine precisely the degree of distortion with the constrained seam carving, we calculated shifts in the 50-th and 100-th rows of Figure 3(c) which are depicted in Figure 4(b). As can be observed, the pixel shifts in Figure 4(b) have been bounded to within $\pm 1$ pixel as expected, contrasting significantly to the 15 pixel shift in Figure 4(a). Moreover, the shifts in Figure 4(b) are not cumulative as opposed to those in Figure 4(a) and exhibit random properties, which more or less mitigate the effect of the distortion generated by seam operations.

## IV. RESULTS

Figure 3(c) and 4(b) illustrate that the constrained seam carving reduces significantly the level of geometrical distortion introduced by seam operations. In this section, we present results to illustrate content-adaptive ability of the constrained seam carving method. Figure 6 shows the results of 5% expansion of the test image in Figure 2(a) using nearest neighbour mapping and the constrained seam carving. It can be seen the constrained seam carving generates irregular aliasing which appears less intrusive than the regular aliasing generated by the nearest neighbor mapping. This result confirms that constrained seam carving is indeed able to be aware of image contents and alter the image accordingly.

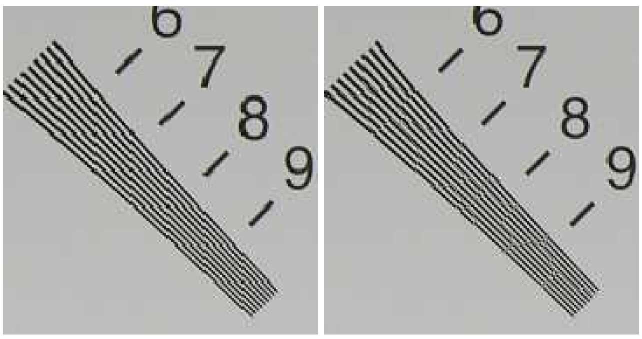


(a) (b)

Figure 6 Comparison between nearest neighbor mapping (a) and constrained seam carving (b) using the test image in Figure 2(a)

Figure 7 gives the results from a real cine image. It can be seen that nearest neighbour mapping generated clearly noticeable artifacts, e.g. in the lip, nose and cheek areas in Figure 7(b). In contrast, the artifacts are well hidden in Figure 7(c), where the seam carving technique finds low energy paths (which are not sensitive to human eyes) to replicate pixels.

(a) A real cine image

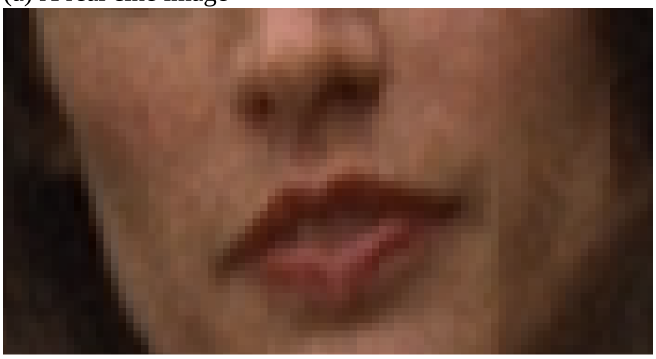

(b) Result by nearest neighbour mapping

(c) Result by constrained seam carving

Figure 7 Comparison between nearest neighbour mapping (b) and constrained seam carving (c) using a real cine image (a)

## V. CONCLUSIONS

This paper discusses fractional image rescaling in digital cine applications. It is found that image degradation is inevitable in fractional image rescaling and that the degradation can be transformed by incrementing the warping function that represents an image rescaling operation with a displacement map. Based on this idea, a constrained seam carving method is devised to adjust the displacement map to alter the aliasing present in the rescaled image according to the original image contents. Our experimental results confirm that this technique is able to rescale images adaptively according to their contents while preserving the geometry of the image contents globally in a linear manner. Application of this method to real cine sequences is currently ongoing.

## References


[1] S. Avidan and A. Shamir, "Seam Carving for Content-Aware Image Resizing," *ACM Transactions on Graphics*, vol. 26, 2007.

[2] G. Wolberg, *Digital Image Warping*. Los Alamitos: IEEE Computer Society Press, 1994.

[3] E. H. Adelson, C. H. Anderson, J. R. Bergen, and P. Burt, "Pyramid methods in image processing," *RCA Engineers*, vol. 29, pp. 33-41, 1984.

[4] C. Zhang and T. Chen, "A survey on image-based rendering—representation, sampling and compression," *Signal Processing: Image Communication*, vol. 19, pp. 1-28, 2004.

[5] A. P. Witkin, "Scale-space filtering," in *Readings in computer vision: issues, problems, principles, and paradigms*, *Morgan Kaufmann Readings Series*. San Francisco: Morgan Kaufmann Publishers Inc., 1987, pp. 329 - 332.

[6] M. Elad and A. Feuer, "Restoration of Single Super-Resolution Image from Several Blurred, Noisy and Down-Sampled Measured Images," *IEEE Transactions on Image Processing*, vol. 6, pp. 1646-1658, 1997.

[7] T. Huang and R. Tsai, "Multi-Frame Image Restoration and Registration," in *Advances in Computer Vision and Image Processing*, vol. 1, 1984, pp. 317-339.

[8] W. T. Freeman, T. R. Jones, and E. C. Pasztor, "Example-Based Super-Resolution," *IEEE Computer Graphics and Applications*, pp. 56-65, 2002.

[9] C. Liu, H. Y. Shum, and C. S. Zhang, "A two-step approach to hallucinating faces: Global parametric model and local nonparametric model," presented at IEEE Conf. Computer Vision and Pattern Recognition, 2001.

[10] H. Wendland, "Gaussian interpolation revisited," in *Trends in Approximation Theory*, K. Kopotun, T. Lyche, and M. Neamtu, Eds. Nashville: Vanderbilt University Press, 2001, pp. 427-436.

[11] L. P. Yaroslavsky, "Efficient algorithm for discrete sinc interpolation," *Applied Optics*, vol. 36, pp. 460-463, 1997.

[12] H. S. Hou and H. C. Andrews, "CUBIC-SPLINES FOR IMAGE INTERPOLATION AND DIGITAL FILTERING," *IEEE TRANSACTIONS ON ACOUSTICS SPEECH AND SIGNAL PROCESSING*, vol. 26, pp. 508-517, 1978.

[13] N. A. Dodgson, "Quadratic interpolation for image resampling," *IEEE Transactions on Image Processing*, vol. 6, pp. 1322-1326, 1997.

[14] T. M. Lehmann, C. Gonner, and K. Spitzer, "Survey: Interpolation methods in medical image processing," *IEEE Transactions on Medical Imaging*, vol. 18, pp. 1049-1075, 1999.

[15] Q. Wang and R. K. Ward, "A New Orientation-Adaptive Interpolation Method," *IEEE Transactions on Image Processing*, vol. 16, pp. 889-900, 2007.

[16] L. Zhang and X. Wu, "An Edge-Guided Image Interpolation Algorithm via Directional Filtering and Data Fusion," *IEEE Transactions on Image Processing*, vol. 15, pp. 2226-2238, 2006.

[17] P. V. Sankar, "SIMPLE ALGORITHMS AND ARCHITECTURES FOR B-SPLINE INTERPOLATION," *IEEE TRANSACTIONS ON PATTERN ANALYSIS AND MACHINE INTELLIGENCE*, vol. 10, pp. 271-277, 1988.

[18] Y. L. Huang, "Wavelet-based image interpolation using multilayer perceptrons," *Neural Computing and Applications*, vol. 14, pp. 1-10, 2005.